Faculty and Researchers   Faculty and Researchers' Publications

2015-06

Optimizing detection methods for terahertz bioimaging applications

Karunasiri, Gamani; Grbovic, Dragoslav; Karanasiou, Irene S.; Bolakis, Christos; Uzunoglu, Nikolaos

SPIE

Optimizing detection methods for terahertz bioimaging applications

Christos Bolakis
Irene S. Karanasiou
Dragoslav Grbovic
Gamani Karunasiri
Nikolaos Uzunoglu

SPIE.

Optimizing detection methods for terahertz bioimaging applications

Christos Bolakis,[a,*] Irene S. Karanasiou,[b] Dragoslav Grbovic,[c] Gamani Karunasiri,[c] and Nikolaos Uzunoglu[b]
[a]National Technical University of Athens, School of Electrical and Computer Engineering, 9 Heroon Polytechniou, Zografou 15780, Greece
[b]National Technical University of Athens, Institute of Communication and Computer Systems, 9 Heroon Polytechniou, Zografou 15780, Greece
[c]Naval Postgraduate School, Department of Physics, 1 University Circle, Monterey, California 93943, United States

Abstract. We propose a new approach for efficient detection of terahertz (THz) radiation in biomedical imaging applications. A double-layered absorber consisting of a 32-nm-thick aluminum (Al) metallic layer, located on a glass medium (SiO_2) of 1 mm thickness, was fabricated and used to design a fine-tuned absorber through a theoretical and finite element modeling process. The results indicate that the proposed low-cost, double-layered absorber can be tuned based on the metal layer sheet resistance and the thickness of various glass media. This can be done in a way that takes advantage of the diversity of the absorption of the metal films in the desired THz domain (6 to 10 THz). It was found that the composite absorber could absorb up to 86% (a percentage exceeding the 50%, previously shown to be the highest achievable when using single thin metal layer) and reflect <1% of the incident THz power. This approach will enable monitoring of the transmission coefficient (THz transmission fingerprint) of the biosample with high accuracy, while also making the proposed double-layered absorber a good candidate for a microbolometer pixel's active element. © 2015 Society of Photo-Optical Instrumentation Engineers (SPIE) [DOI: 10.1117/1.OE.54.6.067107]

Keywords: terahertz; bioimaging; fine-tuned absorber; fingerprint; microbolometer.

Paper 150262 received Mar. 3, 2015; accepted for publication May 27, 2015; published online Jun. 22, 2015.

1 Introduction

Much research focuses on the terahertz (THz) frequency region, which lies between the microwave and the infrared electromagnetic spectra, ranging from ∼0.1 to 10 THz. This region remained unexplored until the last decade due to the lack of sufficiently compact and efficient sources and detectors. However, new, promising THz applications, including biomedicine, homeland-security, telecommunications, and astronomy, in conjunction with the considerable technological progress in electronics and optics, have spurred the development of reliable THz components.

THz imaging for biomedical applications has been a trend recently. THz radiation is classified as nonionizing, thus is harmless to biological tissues. Moreover, vibrational and rotational spectra of biomolecules lie in the THz frequency region, giving a distinct THz fingerprint.[1–4] These two properties make THz radiation very appealing for biomedical applications. THz imaging and sensing techniques are already used at medical centers for cancer and burn diagnosis.[5–8] In addition, THz imaging appears particularly suited for examining skin abnormalities, such as skin cancer, as well as characterizing human tissues.[9] Nevertheless, the interaction of biological materials with THz radiation is not completely understood: the THz response of biological samples is considerably affected by specific radiation properties and the experimental configuration as well as sample preparation and measurement procedures. The development of an imaging technique that could identify the unique THz response (THz transmission fingerprint) of a biosample could lead to the generation of a database with unique spectral signatures of biological samples, thus contributing to the systematic use of THz technology for medical diagnostics.

Much progress has been made in both the emitting and detection modules for THz systems. Regarding THz detection, numerous methods and detection devices, such as hot electron bolometers, Schottky diodes, thermal detectors featuring metamaterials, etc.,[10,11] have already been explored and are in use.

Interest in the THz spectral range for imaging applications prompted the fabrication of detectors sensitive in the 100 GHz to 10 THz frequency band. Room temperature detection has also been achieved using bi-material MEMS detector arrays,[12] antenna-coupled photodetectors,[13] nanowire and graphene nanodetectors (which is also the latest development for room temperature THz detectors),[14] or microbolometers.[15–17] Originally developed for infrared wavelengths, the microbolometer detectors were used for imaging in the THz spectral range using illumination from a quantum cascade laser.[16,17] In order to enhance the sensitivity of microbolometer detectors at THz frequencies, it is important to embed strong THz-absorbing layers into microfabricated detectors. It has been shown that thin metal films deposited on dielectrics provide good THz absorption due to resistive losses in the film.[17–19] Moreover, for normal incidence, it has been shown that a free-standing metallic layer can absorb up to 50% of the incident radiation.[20]

In our previous work, we have proposed development of a novel two-dimensional THz imaging system for investigation of brain tissue samples both at the macroscopic and at the biomolecular level.[1] In this paper, we propose new components for the effective detection of THz radiation of

interest; to this end, the design and performance of an effective absorber of radiation that passes through a biosample is presented, with potential application as a component of the detection module of the proposed system.

2 Materials and Methods

2.1 *THz Absorber Setup*

As a continuation of previous work,[18,19] the absorber used in our model was designed as a thin metallic layer located on a glass substrate (SiO_2). Through the usage of such a metal-glass configuration, the transmission of a metal film is the same, regardless of the direction in which it is measured (either the metal or the glass side). This is not the case for reflectance, and if measured at the glass side, reflectance is slightly lower than when measured at the metal side. Since $T + A + R = 1$, the reduction in reflectance at the glass side means that the absorption from that side must always be higher.[21] As a result, by configuring the detector in a way that the incident wave meets the glass layer first and increases its absorption capabilities, it could satisfy some of the requirements (i.e., active element of a microbolometer) of the conventional detection scheme that could be used to measure the THz transmission of the biosample of interest, as illustrated in Fig. 1(a). Under specific spectral characteristics of the source and using the thin metal film with an appropriate thickness and conductivity, one can obtain zero reflectivity and high THz absorption. The absence of bounce-back radiation from our absorber, used as a part of the detector in a configuration illustrated in Fig. 1(a), implies that the transmission properties (THz transmission fingerprint) of the specimen can be efficiently obtained by our double-layered (metal and glass) absorber. Such properties can be key in distinguishing between healthy and diseased biotissue samples as explicitly described in Ref. 22. A measurement of the corresponding resistive heating of the metal layer could quantify that absorption. In addition, measurement could be performed through a microbolometer by allowing the described double-layered absorber to be its respective absorbing element. The THz characteristics of the absorber were modeled using the analytical approach described in Ref. 23 as well as by finite element modeling using COMSOL Multiphysics software.

2.2 *Analytical Approach*

Absorption of electromagnetic radiation in a thin metal film located on a glass medium (SiO_2) can be calculated by determining transmission and reflection and taking into account multiple reflections in each interface of the double-layered absorber as explicitly described in Refs. 23 and 24 and illustrated in Fig. 1(b). The absorption is then estimated by subtracting transmission and reflection from the unity.

While the index of refraction of the SiO_2 that was used for our analysis was 1.46, the frequency-dependent index of refraction of the metal thin film can be described by Eq. (1).[24] The complex nature of the index of refraction reflects the absorptive nature of the metal layer. The absorption of the incoming radiation will depend on the conductivity (σ) of the metal.

$$n = (1 - i)\sqrt{\frac{\sigma}{4\pi\varepsilon_0 f}}, \tag{1}$$

where f is the frequency of incident radiation and σ is the film conductivity.

Moreover, the reflection and transmission coefficients can be obtained using the following recursive equations:[23,24]

$$r_i = \frac{r_{i-1,i} + r_{i+1}e^{-2j\varphi_i}}{1 + r_{i-1,i}r_{i+1}e^{-2j\varphi_i}} \tag{2}$$

$$t_i = \frac{t_{i-1,i}t_{i+1}e^{-j\varphi_i}}{1 + r_{i-1,i}r_{i+1}e^{-2j\varphi_i}}, \tag{3}$$
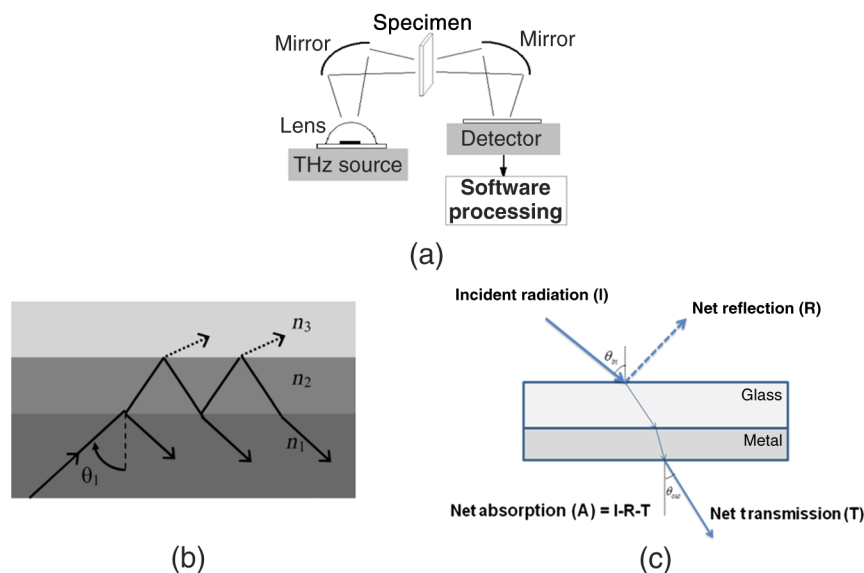

Fig. 1 (a) General detection scheme of the specimen's transmission measurement and (b) three-layer structure used in calculation of transmission and reflection (from Ref. 23). Medium 1 is air, medium 2 is SiO_2, and medium 3 is a thin metal layer. (c) Schematics of the specific simulated area of the modeled double-layered absorber through COMSOL finite elements software.

where r_i and t_i are the total coefficients of reflection and transmission, respectively, from the i'th layer and above, $r_{k,m}$ and $t_{k,m}$ are the Fresnel coefficients of reflection and transmission, respectively, and φ_i is the phase change when propagating through layer i. Such a phase change is given by

$$\varphi_i = \frac{2\pi}{\lambda} n_i d_i \cos \theta_i, \qquad (4)$$

where λ is the free space wavelength, n_i is the index of refraction of layer i, d_i is the thickness of layer i, and θ_i is the associated term of the Snell's law.

If total reflection of the double-layered absorber [fraction of the incoming power reflected from layers 2 and 3 from Fig. 1(b)] is $rr*$ and the transmission [fraction of the incoming power transmitted from layers 2 and 3 from Fig. 1(b)] is $(\cos \theta_{out} / \cos \theta_{in}) tt*$, where θ_{in} and θ_{out} are the angles of incidence and transmission, respectively, then by subtracting the reflection and transmission coefficients from the unity, absorption in the absorber can be obtained as

$$A = 1 - rr* - \frac{\cos \theta_{out}}{\cos \theta_{in}} tt*. \qquad (5)$$

2.3 Finite Element Modeling

The THz characteristics of the double-layered absorber were also simulated using COMSOL Multiphysics finite element modeling software.[25] The main advantage of COMSOL is that it provides a convenient way to determine absorption in individual layers of the absorber structure. This is useful when several layers, in addition to the substrate, absorb the incident radiation. The analytical approach described above also provides a way to compare the validity of the simulation. Before modeling using COMSOL, it is important to set appropriate physics and boundary conditions in addition to the physical dimensions of the layer structure in the absorber.

Designing the model illustrated in Fig. 1(c) and following the solving path as explicitly described in Ref. 26, the THz absorption can be directly estimated by integrating the resistive heating power in the subdomain that corresponds to the metal layer of the double-layered absorber.

3 Results

The results presented in this section are twofold: initially, the simulation tools are validated by comparing theoretical and experimental results; subsequently, the simulation tools are used to optimize film parameters. In the first part, the measurements lie in the 6- to 10-THz frequency region, chosen due to available experimental measurement capabilities and suitability of the region for THz biomedical applications,[27] while in the latter, simulation results are also presented in the 6- to 10-THz frequency band along with the frequency tuning capability.

3.1 Validation Process Through Experimental Data

As mentioned in Sec. 2.1, under specific spectral characteristics of the source and using thin metal film and glass layers of the double-layered absorber with appropriate thickness and conductivity, one can obtain zero reflectivity. In order to initiate a fine-tuning process involving the parameterization of the quantities of interest (i.e., thickness, conductivity, and frequency of the incident THz radiation), we compared the reflectance results obtained through COMSOL model with experimental measurements.

The characterization of reflectivity of the fabricated double-layered absorber was performed in the 6- to 10-THz spectral band using a Fourier transform infrared spectrometer (FTIR Nexus 8700) fitted with a globar source, Si beam-splitter, and a pyroelectric detector as explicitly described in Ref. 12. The double-layered absorber consisted of a 32-nm-thick aluminum (Al) film with a conductivity of 3.85×10^6 (S/m) and a glass substrate (SiO_2) of 1 mm thickness and refractive index of 1.46. The blue line in Fig. 2 shows the modeled reflection for the double-layered absorber as a function of frequency and the red line shows the experimental reflection, indicating a good agreement between the two. The lack of interference fringes in the experimental data is probably due to some loss mechanism in the substrate, which we were unable to account for. Based on this comparison, it can be stated that it is safe to use the developed model for the desired fine-tuning process regarding our following analysis.

3.2 Fine-Tuning Process

Focusing on defining a margin of the metal's sheet resistance in the double-layered absorber with maximum absorption and minimum reflection, a fine-tuning process can be conducted. The conductivities for various thicknesses of thin Cr films were taken from Ref. 19. Working on a theoretical basis for the fine-tuning process (which will later be verified through the model) and focusing at the frequency of 6 THz, the parameters kept fixed were the Cr thickness of 30 nm [with a conductivity of 0.9×10^6 (S/m), Ref. 19] and the refractive index of the glass medium of 1.46. Through the first step of that process, it was found that for the same metal conductivity [0.9×10^6 (S/m)], the minimum reflection achievable as a function of the glass thickness around 5 μm was 45% at 8.5 μm (i.e., instead of 60% at 5 μm). A synopsis of the above process is given in Table 1.

Moving on to the second (and final) step and preserving the glass thickness at 8.5 μm, we reiterated the process, now

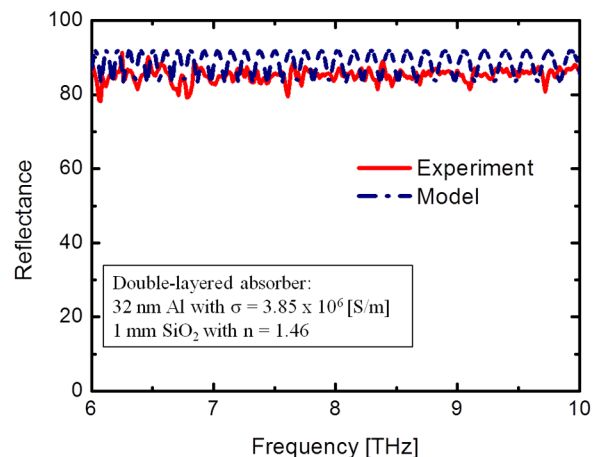**Fig. 2** Modeled versus experimental reflection of the double-layered absorber as a function of frequency.

Table 1 Numerical synopsis of the first step of the fine-tuning process.

| Fixed values	Variable values	Results
Cr thickness = 30 nm	SiO$_2$ thickness: 1 to 10 μm	Minimum possible reflection (45%) for SiO$_2$ thickness = 8.5 μm
Cr conductivity = 0.9 × 106 (S/m)		
SiO$_2$ refractive index = 1.46		
Frequency of incidence = 6 THz		

varying the metal's sheet resistance (R_s) from 1 to 1500 ($\Omega/\square$). Such variation was conducted through respective variation of the thickness of the thin metal Cr layer. The definition of the sheet resistance states

$$R_s = \frac{1}{\text{conductivity} * \text{thickness}}. \qquad (6)$$

By assuming a linear dependence of the conductivity on thickness (i.e., $\sigma = At + B$, where A and B are constants dependent on the type of the metal and can be defined through the linear fitting process) and using the reported data for the measured conductivities from Ref. 19, the sheet resistance was defined as a function of an inverse square of the metal thickness. That sheet resistance was inserted into the Rouard method described in Ref. 23. From Eq. (1), the index of refraction of the metal of interest could now be expressed as

$$n = (1 - i)5.475\sqrt{\lambda(At + B)}, \qquad (7)$$

where λ is the wavelength of the incident radiation. All calculations were conducted for normal incidence. The resulting reflection, transmission, and absorption are displayed in Fig. 3. Moreover, the calculated absorption was also
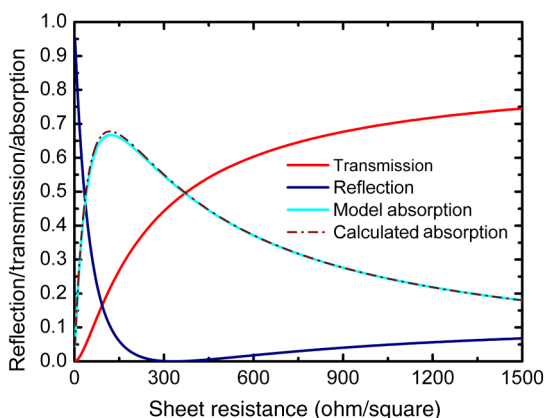
Fig. 3 Calculated reflection and transmission coefficients, model and calculated absorption of the double-layered absorber as a function of sheet resistance at 6 THz.

compared with the modeled one, indicating excellent agreement between the two approaches.

It can be seen from the above figure that for a sheet resistance of ~300 ($\Omega/\square$) (8 nm thickness for Cr), we get nearly zero reflectance. Moreover, we also get 40% transmission and 60% absorption of the incident THz radiation. Specifically, the sheet resistance margin where we get <1% reflection and >50% absorption is from 240 to 370 ($\Omega/\square$) with 60 and 50% absorption, respectively. A percentage exclusively representing the absorption from the thin metal layer (after verification through COMSOL Multiphysics finite element modeling software), which is greater than the one demonstrated in our previous work and which was up to 50%,[18,19] has been shown to be the maximum achievable for a free standing metal film.[20] Moreover, as can be seen from Fig. 3, there is also a sheet resistance value around 150 ($\Omega/\square$), where higher absorption is achievable (a little less than 70%) but with a 10% reflection. In order to counter balance the absorption and the reflection capabilities of our double-layer absorber, the following analysis will take place in the margin from 240 to 370 ($\Omega/\square$]. In Sec. 4, we will show that the highest possible absorption will be always followed with almost zero reflectance.

The predefined sheet resistance margin can be generalized for any thin metal film. The conductivity of the thin Cr film used could be expressed as $\sigma = At + B$, where A and B are constants that are dependent on the type of the metal. From Ref. 19, the calculated A and B through linear fit processing were found to be 2.192×10^{13} (S/m^2) and 2.423×10^5 (S/m), respectively. Furthermore, we reiterated the process for a thin Ni film. Again from Ref. 19, we calculated the arbitrary constants A' and B' ($\sigma = A't + B'$) for Ni, which came out to be 5.053×10^{13} (S/m^2) and 3.074×10^6 (S/m), respectively. Ultimately, it was shown that at the fixed frequency of 6 THz and a fixed glass thickness of 8.5 μm, the sheet resistance where we get nearly zero reflectance was identical for both Cr and Ni metal films of the double-layered absorber (Fig. 3). This sheet resistance [300 ($\Omega/\square$)] corresponds to the 1 nm Ni film. As a result, the region of 240 to 370 ($\Omega/\square$) should be achievable with any thin metal film. However, each material will achieve those values at different thicknesses. A synopsis of the above process is given in Table 2.

In summary, a glass layer (SiO$_2$) of thickness 8.5 μm and refractive index of 1.46 adjusted to any thin metal film with a sheet resistance from 240 to 370 ($\Omega/\square$) resulted in a double-layered absorber, which is capable of absorbing 60 and 50%

Table 2 Numerical synopsis of the final step of the fine-tuning process.

Fixed values	Variable values	Results
SiO$_2$ thickness = 8.5 μm	Sheet resistance of any metal: 1 to 1500 ($\Omega/\square$]	Maximum possible absorption (60%) with almost 0% reflection for any metal with a sheet resistance of 240 ($\Omega/\square$)
SiO$_2$ refractive index = 1.46		
Frequency of incidence = 6 THz		

of the incident radiation of 6 THz, respectively. These percentages surpass the 50% limitation discussed earlier.

The model indicates that the use of four successive sets of the double-layered absorber would result in an ~100% absorption. Specifically, a metal sheet resistance of 240 ($\Omega/\square$) would provide reflection and transmission of ~1% each, respectively, and 98% absorption (as shown in Fig. 4). The finite element model could also determine the distribution of absorbed power in individual layers.

3.3 Frequency Dependence and Frequency Tuning

Due to our interest in examining the absorption characteristics of the double-layered absorber as a function of frequency, we calculated the reflection as a function of frequency covering the whole THz spectrum (from 0.1 to 10 THz). We kept the parameters of the glass medium (SiO_2) fixed and we picked the sheet resistance for the metal film of 240 ($\Omega/\square$). This value, as indicated in Fig. 3, provides the highest absorption (60%) and <1% reflection. As illustrated in Fig. 5, those absorption and reflection values stay at those values only close to 6 THz.

As we plan to experimentally study biomolecule vibrational and rotational spectra in the THz frequency band from 6 to 10 THz, the analysis of reflection, transmission, and absorption of the developed double-layered absorber was performed in that region and the results are illustrated in the inset of Fig. 5.

As seen, there is an optimum region near the central frequency of 6 THz (from 6 to ~7 THz) that gives the same result (i.e., <1% reflection and ~60% absorption). Further analysis could be focused on the effort to define a parameter that would allow tuning of the optimal frequency region in order to cover all the spectrum of interest from 6 to 10 THz. Such a parameter could be the glass layer thickness.

Modeling different glass thicknesses, it was found that a 3 μm decrease of that thickness would cause an ~3 THz shift of the optimum frequency region to the right (higher frequencies). In order to analyze the overall shift from the glass layer thickness decrease, the thickness was iterated in four 0.75-μm steps. The results for all steps, including the reflection of the default double-layered absorber with the glass layer of 8.5 μm, are illustrated in Fig. 6 (only the reflection coefficient is shown).
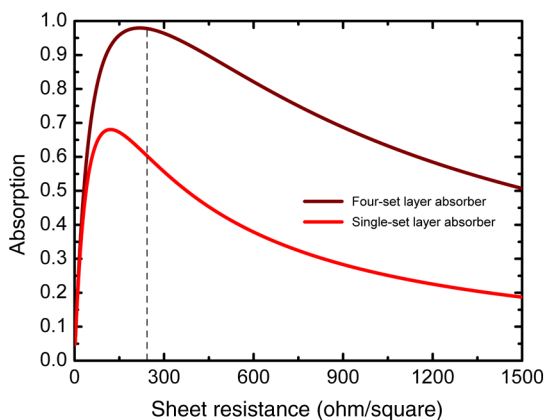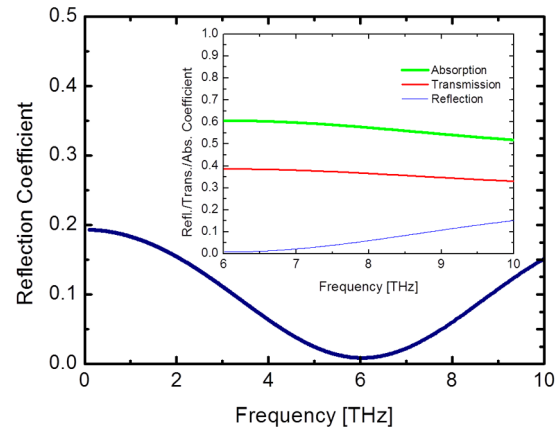

Fig. 5 Calculated reflection of the double-layered absorber as a function of frequency and the calculated reflection, transmission, and absorption of the double-layered absorber as a function of frequency of interest from 6 to 10 THz (inset).

As it can be seen from Fig. 6, there are optimum frequency regions (regions from 1 to 5 with high absorption and low reflection) in the spectrum of interest (from 6 to 10 THz). These regions exhibit a reflection of 1% and an absorption of 60% (not shown in Fig. 6). Any of the five optimum frequency regions could be selected by simply choosing the corresponding discrete glass thickness of the double-layered absorber (from 8.5 to 5.5 μm).

4 Material Inspection

Until now, all the fine-tuning involved variations of the thickness of the glass and metal layer at a fixed frequency. Afterward, those results were examined for a frequency region of interest. Further inspection of the glass layer would be of great interest. There are numerous values reported for the indices of refraction of different types of glass in the THz regime.[28] A similar analysis for each refractive index took place in order to define the sheet resistances that provide almost zero reflection with the highest absorption. The results are given in Table 3.

As can be seen from Table 3, by adjusting the metal's sheet resistance and glass thickness at a higher refractive index of glass, a higher absorption can be obtained. Assuming that the index of refraction 2.52 of BK 7 is the highest possible for a glass material in the THz regime, the values of thickness and sheet resistance are the smallest

Fig. 4 Absorption of the single-set versus four-set double-layered absorber at 6 THz as a function of sheet resistance.
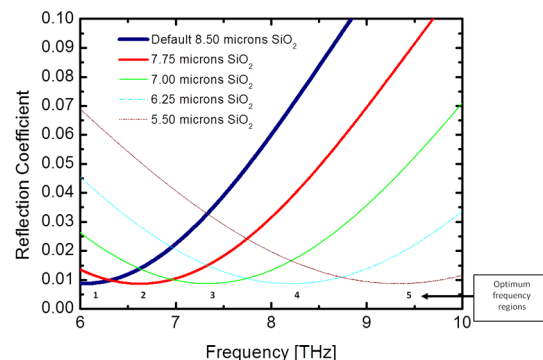

Fig. 6 Calculated shift of the reflection coefficient of the double-layered absorber as a function of the frequency of interest.

Table 3 The highest achievable absorption (with almost zero reflection) for specific values of metal sheet resistance and glass thickness for each type of the referred glass.

Type of glass	Refractive index (Ref. 23)	Thickness (μm)	Metal's sheet resistance (Ω/square)	Absorption (%)
SiO$_2$ (default)	1.46	8.5	240	60
Polycrystalline quartz or amorphous silica	1.96	6.2	105	78
Pyrex	2.11	5.9	85	81
BK 7	2.52	4.9	55	86

while achieving the highest absorption. Similar to the results in Fig. 4, the use of a four set (instead of two in the case of glass) of the developed double-layer absorber could lead to an ~100% absorption. As with glass, the frequency tuning capability is preserved for BK 7, as illustrated in Fig. 7.

5 Integration to a Microbolometer

To date, there exist a variety of materials that are used for the detector element in microbolometers. The pixel's sensitive region is a thin membrane jointly composed of an absorbing layer and a high temperature coefficient of resistance (TCR) layer (i.e., VOx).[29] For every material that is used, it is desirable to conform to standards, such as the ability for integration with CMOS in relatively low temperatures and low $1/f$ noise.[30] The noise equivalent temperature difference of state-of-the-art uncooled bolometers is typically limited by the $1/f$ noise from the bolometer's temperature sensing material.[31,32] In addition, these two standards are fully satisfied by using thin metal layers as the active pixel element. On the other hand, the low TCR of metals constrains the wide usage of such films.

Two of the most critical metrics for any thermal detection system is its voltage responsivity and the root mean square of its sensitivity. Assuming that the pixel temperature
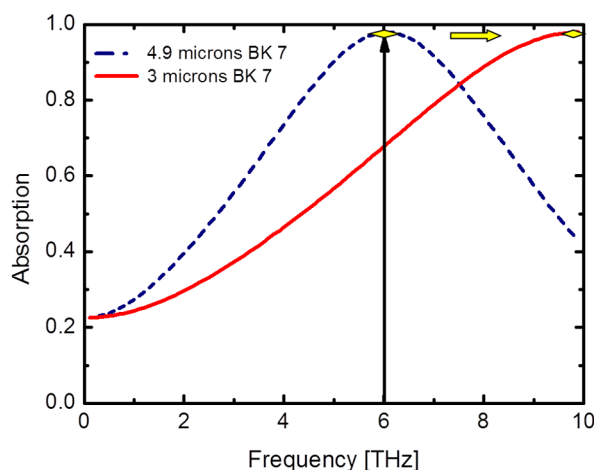

Fig. 7 Calculated shift of the absorption of the double-layered absorber as a function of frequency of interest for multiple BK 7 thicknesses.

sinusoidally increases and decreases with the same frequency at which the input power is modulated, the above quantities will be given, respectively, from the following equations:[16]

$$R_v = \frac{i_b a R \eta}{G\sqrt{1+\omega^2\tau^2}}, \tag{8}$$

$$\Delta T_{\text{RMS}} = \frac{\eta P_o}{G\sqrt{1+\omega^2\tau^2}}, \tag{9}$$

where i_b is the bias current, a is the temperature coefficient of resistance, R is the initial microbolometer's resistance, η is the fraction of incident radiation that is actually absorbed by the pixel's sensitive layer, G is the thermal conductance of the pixel, ω is the modulating frequency, P_o is the incident power, and τ is the time constant of the detector.

From the above equations, the significance of G, η, and a is obvious. More specifically, the choice of a metal (i.e., titanium) of low thermal conductivity increases both the responsivity and sensitivity of the thermal detector. In addition, η plays a dominant role in overall sensitivity and responsivity performance of the detector. In previous work, it has been shown that thin metal films deposited on dielectrics provide good THz absorption due to resistive losses in the film.[17] As a result, 50% of THz absorption is achievable.[18] This is the highest absorption achievable for a thin metal film of any thickness and conductivity.[19,20]

Focusing now on the double-layered absorber (thin metal layer—glass with an index of refraction of 2.52), it can be seen that a THz absorption up to 86% is feasible. Moreover, contributing to the simplicity of the fabrication process, the relative fabrication of an optical resonant cavity for increased absorption[33,34] does not seem appealing, given that the increase in absorption due to the fine-tuning process will be much greater than the increase due to the cavity.

In conclusion, considering the importance of the two requirements (CMOS integration and low $1/f$ noise) for microbolometer design, the optimal performance of the double-layered absorber (<1% reflectance and 86% absorption) and the capability of frequency tuning from 6 to 10 THz, the proposed double-layered absorber could be considered as an important candidate for a microbolometer pixel's active element.

6 Discussion and Conclusion

In this paper, recent THz detection results were presented for a double-layered absorber of a thin metallic layer located on a glass medium. The THz absorption characteristics were calculated and modeled. Excellent agreement between theory and simulation shows that modeling can be used for optimizing the parameters to achieve maximum absorption and minimum reflection of such detection structures in THz range. We propose a low-cost, double-layered absorber, optimized through the appropriate parameterization, covering the THz domain (from 6 to 10 THz) for biomedical applications (THz transmission fingerprint evaluation). If implemented as an effective absorbing element of a microbolometer, it could accurately measure the transmission of the biosample under examination. This method allows preserving the benefits of using thin metal layers as bolometric active pixel elements and simultaneously, through an

optimization process, significantly increased absorption (to >50%), a percentage that cannot be exceeded by a single thin metal layer.[18–20]

Future research optimizing the microbolometer performance could be focused on the optimization of the TCR for the double-layered absorber. Given the fact that for every metal glass film combination there will be a sheet resistance that gets nearly zero reflectance and the highest possible absorption, a domain could be defined to optimize the TCR (i.e., the highest possible). Such techniques have already been conducted.[35] As a result, through that multioptimization process, the microbolometer detector efficiency could be further improved.

References

1. P. Bakopoulos et al., "A tunable continuous wave (CW) and shortpulse optical source for THz brain imaging applications," *Meas. Sci. Technol.* **20**, 104001 (2009).
2. S. J. Oh et al., "Molecular imaging with terahertz waves," *Opt. Express* **19**, 5 (2011).
3. M. Gretel et al., "Terahertz spectroscopic differentiation of microstructures in protein gels," *Opt. Express* **17**, 15 (2009).
4. V. P. Wallace et al., "Terahertz pulsed imaging and spectroscopy for biomedical and pharmaceutical applications," *Faraday Discuss.* **126**, 255–263 (2004).
5. M.-A. Brun et al., "Terahertz imaging applied to cancer diagnosis," *Phys. Med. Biol.* **55**, 4615 (2010).
6. P. C. Ashworth et al., "Terahertz pulsed spectroscopy of freshly excised human breast cancer," *Opt. Express* **17**, 12444–12454 (2009).
7. R. M. Woodward et al., "Terahertz pulse imaging of ex vivo basal cell carcinoma," *J. Invest. Dermatol.* **120**, 72–78 (2003).
8. Z. D. Taylor et al., "Reflective terahertz imaging of porcine skin burns," *Opt. Lett.* **33**, 1258–1260 (2008).
9. R. M. Woodward et al., "Terahertz pulse imaging in reflection geometry of human skin cancer and skin tissue," *Phys. Med. Biol.* **47**, 3853–3863 (2002).
10. F. Alves et al., "Microelectromechanical systems bimaterial terahertz sensor with integrated metamaterial absorber," *Opt. Lett.* **37**, 1886–1888 (2012).
11. A. Rogalski and F. Sizov, "Terahertz detectors and focal plane arrays," *Opto-Electron. Rev.* **19**, 346–404 (2003).
12. D. Grbovic and G. Karunasiri, "Fabrication of bi-material MEMS detector arrays for THz imaging," *Proc. SPIE* **7311**, 731108 (2009).
13. Z. D. Taylor et al., "Analysis of pulsed THz imaging using optical character recognition," *IEEE Sens. J.* **9**, 3–8 (2008).
14. M. S. Vitiello, "High performance semiconductor nanowire and graphene terahertz nanodetectors," presented at *Optical Sensors 2014*, Barcelona, Paper SeTh4B.1, OSA publishing (2014).
15. S. Verghese et al., "Generation and detection of coherent terahertz waves using two photomixers," *Appl. Phys. Lett.* **73**, 3824 (1998).
16. B. N. Behnken, "Real-time terahertz imaging using a quantum cascade laser and uncooled microbolometer focal plane array," PhD Dissertation, Naval Postgraduate School, Monterey, CA (2008).
17. A. W. M. Lee et al., "Real-time imaging using a 4.3-THz quantum cascade laser and a 320 × 240 microbolometer focal-plane array," *IEEE Photonics Technol. Lett.* **18**, 1415–1417 (2006).
18. C. Bolakis et al., "Design and characterization of terahertz-absorbing nano-laminates of dielectric and metal thin films," *Opt. Express* **18**, 14488–14495 (2010).
19. F. Alves et al., "Highly absorbing nano-scale metal films for terahertz applications," *Opt. Eng.* **51**, 063801 (2012).
20. L. N. Hadley and D. M. Dennison, "Reflection and transmission interference filters," *J. Opt. Soc. Am.* **37**, 6 (1947).
21. H. A. Macleod, *Thin-Film Optical Filters*, 3rd ed., Institute of Physics Publishing, Bristol and Philadelphia (2001).
22. G. M. Png, "Terahertz spectroscopy and modeling of biotissue," PhD Thesis, University of Adelaide, School of Electrical and Electronic Engineering, Australia (2010).
23. P. Lecaruyer et al., "Generalization of the Rouard method to an absorbing thin-film stack and application to surface plasmon resonance," *Appl. Opt.* **45**, 8419–8423 (2006).
24. M. Born and E. Wolf, *Principles of Optics*, 7th ed., University of Cambridge, Cambridge (1999).
25. COMSOL AB, *Introductory Tutorial to the RF Module: Periodic Problems & Diffraction Grating*, Palo Alto, CA (2009).
26. C. Bolakis, "High terahertz absorbing nanolaminate metal films for fabrication of micromechanical bi-material THz sensors," MS Thesis, Naval Postgraduate School Monterey, CA (2010).
27. E. J. Parrot, Y. Sun, and E. Pickwell, "Terahertz spectroscopy: its future role in medical diagnoses," *J. Mol. Struct.* **1006**, 66–67 (2011).
28. M. Naftaly and R. E. Miles, "Terahertz time-domain spectroscopy for material characterization," *Proc. IEEE* **95**(8), 1658–1665 (2007).
29. F. Niklaus, C. Vieider, and H. Jakobsen, "MEMS-based uncooled infrared bolometer arrays—a review," *Proc. SPIE* **6836**, 68360D (2007).
30. T. Akin et al., "CMOS-based thermal sensors," *Adv. Micro Nanosyst.* **2**, 280–498 (2005).
31. M. Kohin and N. Buttler, "Performance limits of uncooled VOx microbolometer focal plane arrays," *Proc. SPIE* **5406**, 447–453 (2004).
32. P. W. Kruse, "Can the 300 K radiating background noise limit be attained by uncooled thermal imagers?," *Proc. SPIE* **5406**, 437–446 (2004).
33. E. Mottin et al., "Uncooled amorphous silicon technology enhancement for 25 μm pixel pitch achievement," *Proc. SPIE* **4820**, 200–207 (2003).
34. D. Murphy et al., "Performance improvements for VOx microbolometer FPAs," *Proc. SPIE* **5406**, 531–540 (2004).
35. A. Gaitas et al., "Characterization of room temperature metal microbolometers near the metal-insulator transition regime for scanning thermal microscopy," *Appl. Phys. Lett.* **95**, 153108 (2009).

Christos Bolakis received his MSc degree in physics from the Naval Postgraduate School in 2010. Currently, he is a PhD candidate at the School of Electrical and Computer Engineering of the National Technical University of Athens. His current research interests include the optimization of active absorbing elements of terahertz (THz) radiation that can eventually be used in integrated sensors configurations.

Irene S. Karanasiou is a senior researcher in the Institute of Communication and Computer Systems of the National Technical University of Athens. She received her PhD from the National Technical University of Athens, Greece, in 2003, in electrical and computer engineering. Her research interests involve design and development of microwave components and integrated systems, computational electromagnetics, biomedical imaging techniques, and THz radiation applications.

Dragoslav Grbovic received his PhD in physics from University of Tennessee and has done work with IR, THz, and energy harvesting applications. He is experienced with design, microfabrication, and characterization of thin films and metamaterial films for sensing applications.

Gamani Karunasiri received his PhD in physics from the University of Pittsburgh in 1984 and is currently a professor of physics at the Naval Postgraduate School. His current research interests include uncooled THz sensors and imaging systems, MEMS-based directional sound sensors, and solid-state ionizing radiation detectors. He authored or coauthored over 100 publications in refereed journals and holds five U.S. patents.

Nikolaos Uzunoglu is a professor in the School of Electrical and Computer Engineering of the National Technical University of Athens, Greece. He has authored or coauthored over 280 papers in refereed international journals and has authored three books in Greek on microwaves, fiber-optics telecommunications, and radar systems. His research interests include electromagnetic scattering, propagation of electromagnetic waves, fiber-optics telecommunications, and high-speed circuits operating at gigabit/second rates.